JOURNAL OF CIVIL ENGINEERING AND MANAGEMENT
ISSN 1392-3730 print/ISSN 1822-3605 online
2012 Volume 18(5): 701–708
doi:10.3846/13923730.2012.723353

SOIL ARCHING AND LOAD TRANSFER MECHANISM FOR SLOPE STABILIZED WITH PILES

Mehmet Rifat Kahyaoğlu[1], Okan Onal[2], Gökhan Imançlı[3], Gürkan Ozden[4], Arif Ş. Kayalar[5]

Department of Civil Engineering, Muğla University, Kotekli Campus, 48000, Merkez-Muğla, Turkey
E-mails: [1]rifat.kahyaoglu@deu.edu.tr (corresponding author); [2]okan.onal@deu.edu.tr;
[3]gokhan.imancli@deu.edu.tr; [4]gurkan.ozden@deu.edu.tr; [5]arif.kayalari@deu.edu.tr

Received 16 Nov. 2010; accepted 28 Jun. 2011

Abstract. In this study, the effects of pile spacing and pile head fixity on the moment and lateral soil pressure distribution along slope stabilizing piles are investigated. A slice from an infinitely long row of piles with fixed pile tip in an inclined sand bed was simulated with an experimental test setup. Surficial soil displacements were monitored and relative displacements between soil particles were determined by recording time-lapse images during the test in order to observe the soil arching mechanism on the soil surface. The load transfer process from moving soil to piles and behavior of soil around piles were observed and evaluated by the different test setups. It was observed that decrease in pile spacing causes an increase of load carried per pile. This behavior, which was significantly influenced by the pile head boundary conditions, can only be explained by soil arching that existed between the piles along their lengths.

Keywords: slope stabilizing piles, pile spacing, pile head fixity, soil displacement monitoring, soil arching.

1. Introduction

The stabilization of slopes by installing a row of large diameter cast in place reinforced concrete piles has come into widespread use as an effective mean against excessive slope movement in recent years (Sommer 1977; Viggiani 1981; Ito, Matsui 1977; Gudehus, Schwarz 1985; Reese *et al.* 1992; Hong, Han 1996; Poulos 1996; Zeng, Liang 2002; Christopher *et al.* 2007). Stabilizing effect is provided by the passive resistance of the pile below the slip surface and load transfer from the sliding mass to the underlying stationary soil or rock formation through the piles due to soil arching mechanism (Chen *et al.* 1997; Chen, Martin 2002; Liang, Zeng 2002; Ververckaite *et al.* 2007; Kahyaoğlu *et al.* 2009).

Once the excessive movement occurs within the slope above the sliding surface, soil is forced to squeeze between the piles and shear stresses are developed by the relative displacement of the two masses in the interface between the moving and stationary masses. The shearing resistance pretends to keep the yielding mass on its original position by reducing the pressure on the yielding part and increasing the pressure on the adjoining stationary part (Bosscher, Gray 1986; Adachi *et al.* 1989; Pan *et al.* 2000; Cai, Ugai 2003; Zhao *et al.* 2008; Amšiejus *et al.* 2009). This transferring process of forces is called soil arching, which depends on soil properties, pile rigidity, spacing between piles, and relative movement between the soil and the pile, the fixity condition at the pile top (Chelapati 1964; Ladanyi, Hoyaux 1969; Evans 1983; Iglesia 1991).

The formation of the arch is described in terms of major and minor principal stresses of soil. As for isolated piles which subjected to lateral soil movement, radial stresses develop in front of the grouped piles. The difference between isolated piles and grouped piles is that the directions of the major principal stresses from grouped piles do not extend radially from the pile centers, but rather form an arch (Thompson *et al.* 2005). The arch is the path of the major principal stress, and the direction perpendicular to direction of the plane which the minor principal stress acts. The major principal stress increase is still accompanied by a decrease in the minor principal stress.

One of the requirements for practicing soil engineers is to understand the factors influencing the development of soil arching. Incorporating arching mechanism into slope stabilization design requires a comprehensive investigation of the conditions (Poulos 1996; Pan *et al.* 2002; Ždankus, Stelmokaitis 2008; Liang, Yamin 2010).

The focus of the present study is to investigate the load transfer mechanism from sandy soil to slope stabilizing piles and to observe the behavior of the soil around the piles. To this end, a model of a sand slope was established in order to study the effect of pile spacing and pile head fixity condition in one row of piles on the deformation and stress transfer behavior in the system. The bending moment and pressure distribution along the pile length were determined from the deformation of instrumented piles. The soil surface displacements were also monitored and evaluated via digital image analysis techniques in order to observe the soil arching mechanism on the soil surface. Relative displacements between the soil particles were determined by recording time-lapse images.

2. Model test setup

An experimental test setup was designed and manufactured for the investigation of the effects of pile spacing and pile head fixity on the lateral soil pressure. In this setup, a slice from infinite number of piles in an inclined loose sand bed was simulated. The experimental setup consisted of a test box, a pluviation system to prepare homogeneous and uniform loose sand bed, three types of measuring devices such as load cell in front of a loosening support, displacement transducers at model pile heads, strain gages along model piles, and data acquisition systems with 32 channel data logger to digitize and record the information data from measuring devices (Fig. 1).

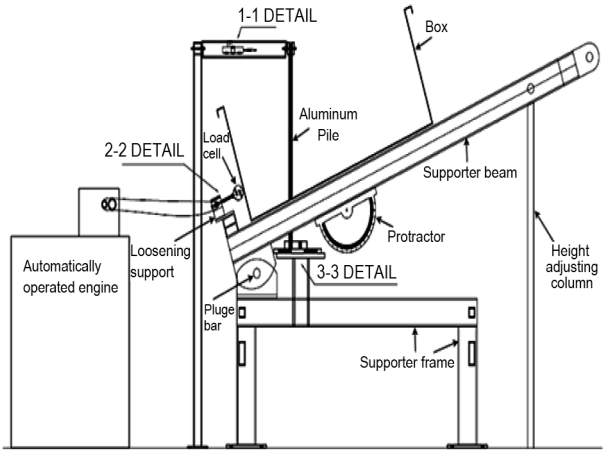

Fig. 1. Section view of experimental setup (Kahyaoğlu 2010)

The test box was made of rigid steel plates. The inside dimensions of test box were 1200 mm in length, 480 mm in width and 500 mm in depth. Two rollers were placed between the direct contact surfaces on two sides. The box was supported from both sides with two 240 cm long steel beams. The test box enables pile tests with fixed pile tip in as many combinations of pile spacing as possible. The model piles used in the tests were made up of aluminum. The length of the solid cylindrical piles was 750 mm with an outside diameter of 20 mm. The bending stiffness of aluminum piles was 5.5×10^5 kNmm^2. Slots of 5 mm in width and 1 mm in depth were sanded smooth and rinsed with acetone along the pile length for mounting strain gages. To obtain the strain and moment behavior of the piles, seven strain gages were directly attached along the pile length perpendicular to the direction of soil movement (Fig. 2). The strain gages were TML FLA-10 model by Tokyo Sokki Kenkyujo Co., with dimensions of 10 mm × 2.5 mm having 8 mm active grid length. The resistance of the gages was 120 Ohms ±0.3%, and the gage factor was 2.090 ± 0.5%. The gages were fixed to the pile with epoxy based glue. The gage resistances were checked prior to installation. After the installation of the gages, the shrink tubes were heated to wrap the pile tightly, covering the strain gages to protect them from mechanical damage during tests. Lateral pile head displacement measurements were measured by utilizing a resistive linear position transducer (RLPT) with 50 mm electrical measuring stroke for sensing the position of an attached pile. Piles were installed along the box perpendicular to the ground and positioned 7.5 times the pile diameter (7.5d) away from the front of the box wall to minimize the end effects (Davie, Sutherland 1978).

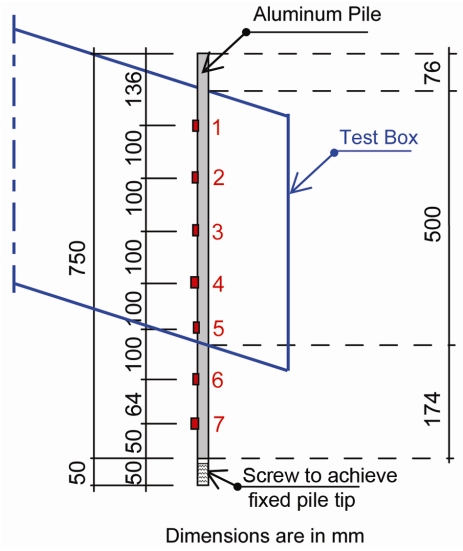

Fig. 2. Instrumentation of piles

Fig. 3 shows the details of the pile installation. The sheet metal with open center for pile installation, was placed between the sliding plane and the box toe (Kahyaoğlu 2010). The centre of the open part of the sheet metal was covered with caoutchouc sheet having holes for pile installation. The diameter of holes was 25 mm and the number of holes was determined according to the pile configuration. The accordion bellow heads were attached to the pile with clamps. The accordion bellows let the pile move freely and prevented the sand to spill during pluviation.

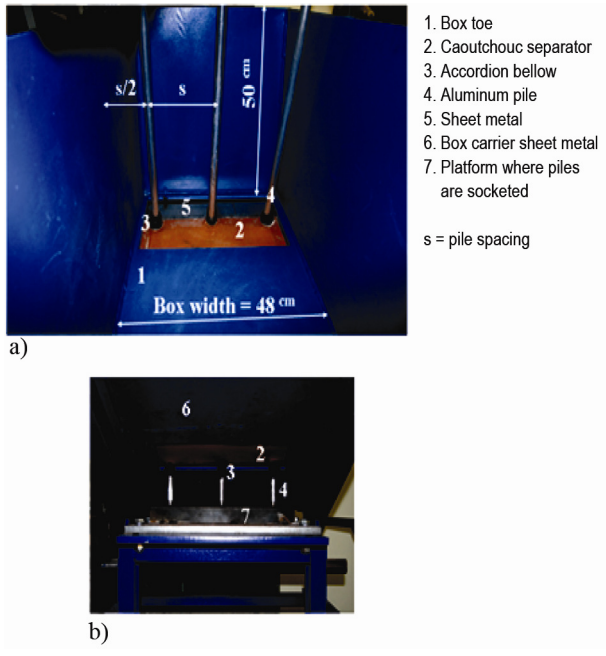

Fig. 3. Photograph of model box with piles: a) Inside view; b) Bottom view

Quartz dry sand was used in testing program to model the granular moving soil. The sand used throughout the experiments was medium to fine sand. The index properties of the sand are given in Table 1.

Table 1. Index properties of the sand

Property	Sand
Mineralogy	Quartz
Specific gravity, G_s	2.65
Mean particle size, D_{50} (mm)	0.50
Maximum and minimum particle size, D_{max}–D_{min} (mm)	0.7–0.3
Coefficient of uniformity, C_u	1.39
Coefficient of curvature, C_c	1.01
Maximum dry density, γ_{max} (Mg/m^3)	0.016376
Minimum dry density, γ_{min} (Mg/m^3)	0.013389
Maximum void ratio, e_{max}	0.98
Minimum void ratio, e_{min}	0.62
Relative density	Loose
Test density, γ_{test} (Mg/m^3)	0.013389
Test void ratio, e_{test}	0.62
Angle of internal friction	32°

In order to create a repeatable and uniform sand bed and to obtain a certain void ratio, a simple deposition device was designed with two basic parts as a reasonable approximation of pluviation method without diffuser meshes. Sand pluviation pan and flexible pipe were utilized to rain the sand into the box. For each experiment, sand deposition was carried out with 2 cm drop height to get a uniform loose sand deposit all over the box. The sand was discharged from the base of the box following the completion of each test, and the box was refilled for the next test.

In the previous studies, researchers set model piles in boxes consisting of two parts (Matsui *et al.* 1982; Cox *et al.* 1983; Chen *et al.* 1997; Nalçakan 1999; Pan *et al.* 2000). The movable upper part of the box was forced by horizontal external load to make uniform horizontal or triangular soil displacement. The fixity effect of the pile in the stationary part was obtained either by a dense soil or a steel plate placed under the sliding surface. However, a landslide is generated by the weight of sliding soil without the influence of any external forces in real. In this study, as a contribution to literature, the movement of the soil was controlled by an automatically operated loosening support to facilitate the soil movement in the downslope direction under its own weight at a constant rate of 2.9 mm/min. The response of the pile was measured and recorded during the box movement until the maximum allowable box displacement was reached (5 cm). Load cell was connected in series to the loosening support for measuring the load-displacement relationships of the box. The friction load (F_r) was computed by subtracting the load measured by the load cell from the sinusoidal component of total weight of box filled with sand in a test without piles. This friction load was taken into account in the interpretation of the test results. The loads acting on the piles were computed by subtracting the friction load from the load measured by load cell. The variations for test program including the pile spacing (s) and the pile head fixity condition were illustrated in Table 2.

Table 2. Test program

Test No	Slope Angle (α)	Pile Spacing (s)	Pile Head Condition	Number of Pile	Number of Repeated Tests
1	20	No pile	–	–	3
2	20	6d	Free head	4	2
3	20	4d	Free head	6	2
4	20	4d	Fixed head	6	3

Tests were repeated two or three times under the same conditions and the results in each series were all found to be very close, with a variation of maximum 5% in total load cell recordings, 8% in transducer recordings and 12% in the strain gage recordings, demonstrating the repeatability of the tests. The bending strain and head displacement values of all piles were the same during the tests so each pile had similar elastic curves. The interpretations on load-displacement relationship were made for the pile in the central position.

Bending strain data were used to generate bending moment vs. depth curves for all tests. These curves present bending moment distributions at successive increments of box displacements. Bending moment measurements provide important information about pile's response. The ultimate bending moment data at the strain gage locations were also best fitted along the pile using Matlab cubic spline interpolation in order to come up with the ultimate bending moment curvature defined as piecewise polynomials.

Distributions of shear force and soil resistance with depth were obtained by successive integration and differentiation of the ultimate bending moment curvature using Matlab cubic spline toolbox. Using spline toolbox, boundary conditions can be applied to the first and second derivative of the spline function. Bending moment values set as zero at the pile head in the case of free head pile. On the other hand, the soil pressure values were set as zero at the soil surface in the case of free and fixed head piles as boundary conditions.

3. Monitoring soil surface displacements

The soil surface displacements were monitored and evaluated via digital image analysis techniques in order to observe the soil arching mechanism on the soil surface. However, since only the top soil surface can be imaged by the camera, the movement of the soil particles below the surface could not be determined. A digital camera was mounted on the test box, which has the same movement with the box and the soil surface to determine the relative surface displacements. The SLR camera Canon 350D with 18–55 mm lens controlled by a laptop computer remotely via USB connection was aligned perpendicular to the inclined surface of the soil (Fig. 4a). The soil surface was equipped with specks having a diameter of 1 mm, in order to measure the relative displacements by monitoring these points (Fig. 4b). The specks were

positioned denser around the piles and become coarser away the piles. Thus, relative displacements between the soil particles were determined by recording time-lapse images throughout the test for 10 seconds time intervals. Time-lapse photography involves taking many pictures of the soil surface over the entire test period and then analyzing them together in order to determine relative soil displacements on the soil surface.

a)

b)

Fig. 4. Position of camera (a); Camera view (b)

The calibration of the camera was performed by imaging a grid paper laid on the soil surface. On the calibration images, 10 mm corresponded to 65 pixels both in vertical and horizontal directions and negligible telecentricity effect was observed. The resolution of the system was determined as 1/6.5 mm. The frame of the camera was arranged so that it captures the zones where soil arching is expected to take place.

4. Digital image processing operations

The image processing and data visualization operations were performed by using MatLab® Technical Computing Language and ImageJ® image analysis software. The relative and final displacements of the monitoring points were marked onto the original soil surface images in order to have a visual explanation of the soil arching phenomena.

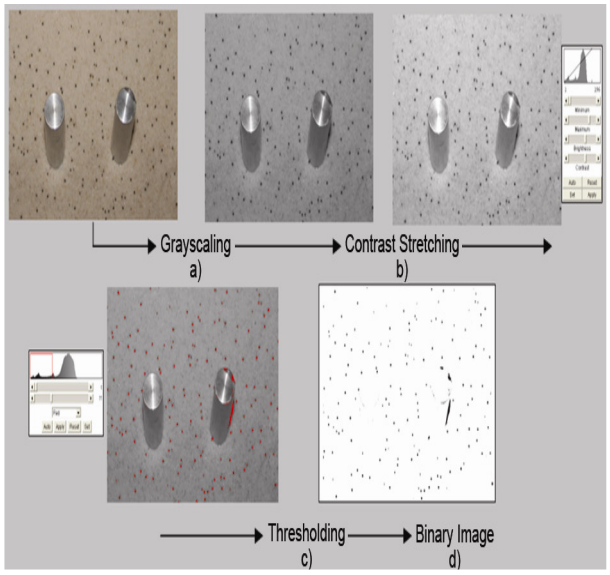

Fig. 5. Digital image processing sequence

The captured images were reduced to 8-bit gray scale images, in order to apply thresholding operation for the segmentation of the displacement tracking points (Fig. 5a). The color of the specks was deliberately chosen as black, resulting relatively low gray values compared to sand particles after gray scaling. However, the contrast between the specks and soil particles was improved by using contrast stretching operation in order to get better segmentation results from the thresholding process (Fig. 5b). The segmentation of the tracking points was performed by choosing a proper threshold value and then applying the thresholding operation (Fig. 5c).The threshold value was determined by using Otsu method (Otsu 1979), which calculates an automated threshold value by using the histogram of the image being used. Thus, pixels having the gray value below the threshold have been converted to black and pixels having the gray value above the threshold converted to white (Fig. 5d).

After the image processing stage, the resulting binary images have been stored for the image analysis in order to determine the coordinates of the segmented tracking points.

5. Digital image analysis

The area and circularity of the segmented tracking points were used as the elimination criteria at the analysis of the binary images. The segmented tracking points were analyzed in the binary images and a discrepancy between the speck areas, varying in a close range interval, was observed. The pixel blocks, having larger area than the speck area interval, were eliminated. Thus, piles, the borders of the box, the tripod were not considered at the analysis. Also, pixel blocks, having less area than the speck area interval, have been eliminated, which ensured the elimination of the mis-threshed pixels and remains of the eliminated big pixel groups. However, the area elimination criteria did not successfully segmented the touching specks alone. Therefore, the circularity of the segmented points was examined. The circularity presents a

quantitative value which is defined as C = (4π area)/(perimeter)^2. A perfect circled speck will have the circularity value of unity, where this value is decreasing according to the distortion of the shape. Since the touching specks have significantly lower circularity values, this pixel blocks were not considered as displacement tracking points in the analysis of the binary images. The centroidal coordinates of the remaining tracking points in each image were determined and stored for the visualization process.

6. Discussion of the test results

6.1. Free head piles

The pile head displacement versus box displacement graphs for free head piles with s/d = 6 and s/d = 4 are shown in Fig. 6. It can be observed from this figure and time lapse images that pile head movement exceeds the soil movement throughout the tests. The relative displacements of the tracking points for free head piles with s/d = 6 and s/d = 4 were shown in Figs 7 and 8, respectively.

For the case of piles with both s/d = 6 and s/d = 4, relative soil movements are seen in the downslope direction. Since the pile pushed the surrounding soil to displace to the down slope direction rather than resisting against sliding. This behavior appears to be distinct in the case of piles with s/d = 4 due to the excess number of piles in the same slice. As seen in these figures, the relative displacements of soil particles decreased with distance from the piles to the upslope direction. One can notice that, if there were no piles, there would not be any relative displacements between the soil particles on the soil surface. The existence of the relative displacements on the soil surface was attributed to the presence of the piles (pile effect). The pile effect became negligible after approximately eight pile diameter (8d) away from the piles. Hence, no relative displacements were determined above this zone during the analysis.

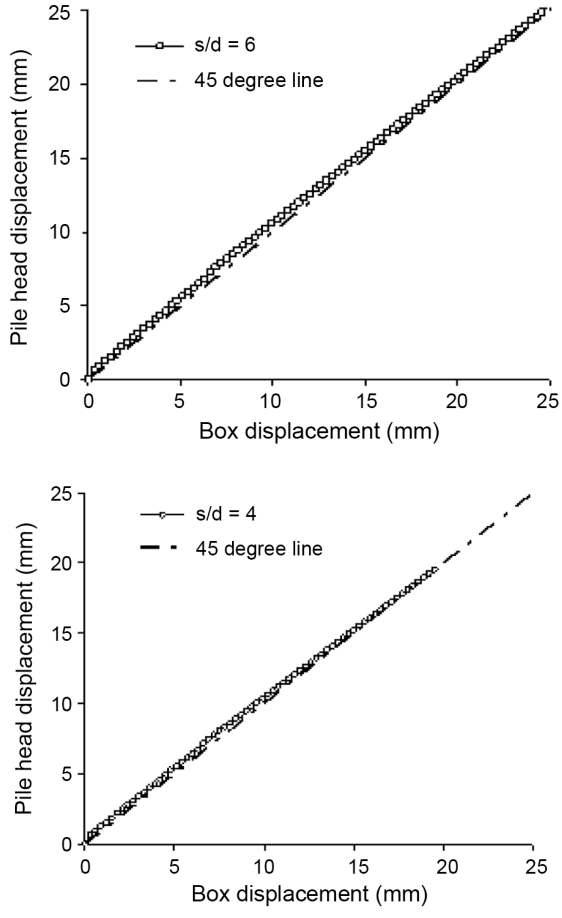

Fig. 6. Pile head displacements versus box displacement

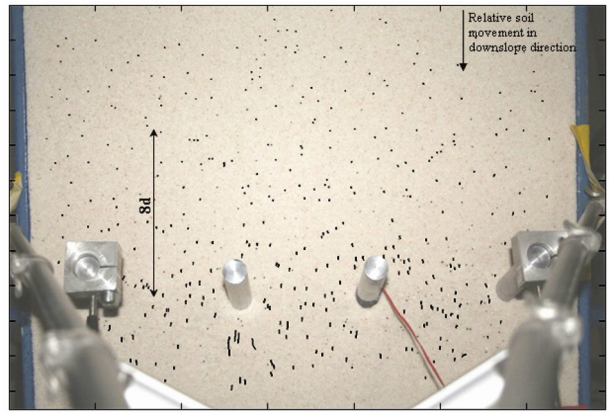

Fig. 7. The overall relative soil surface displacements throughout the test the free head pile test with s/d = 6

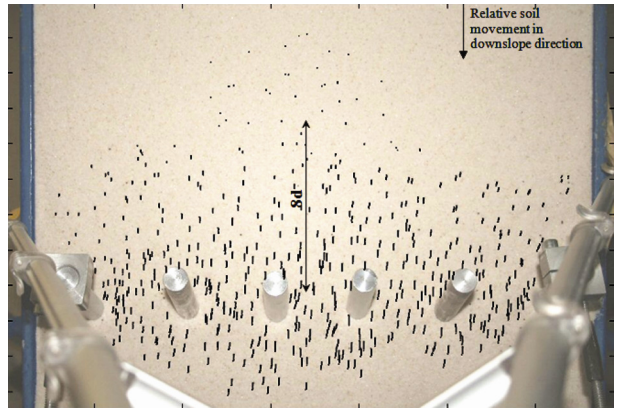

Fig. 8. The overall relative soil surface displacements throughout the test the free head pile test with s/d = 4

The measured load carried by a single pile in a group is shown in Fig. 9. As the displacement of the soil increases, the loads acting on the piles increase rapidly as a result of load transfer mechanism by means of shear. The acting loads reach a maximum value and remain constant as the soil movement continues to increase, when the soil movement reaches a certain value. This indicates that the additional soil movement has no more influence on the load transfer mechanism. It was revealed that the decrease in pile spacing causes an increase of the carried load per pile. This behavior can only be explained by soil arching existed between the piles along the box depth.

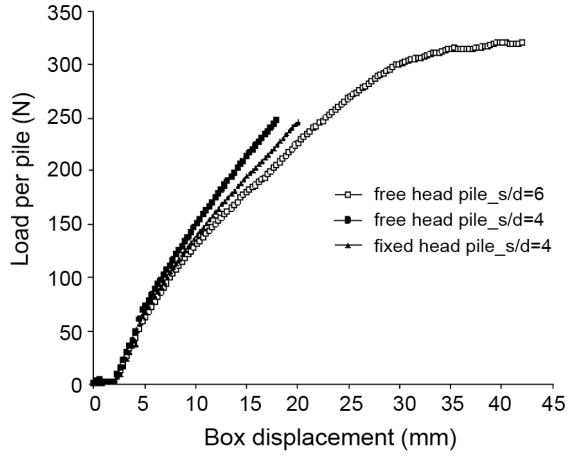

Fig. 9. Load per pile

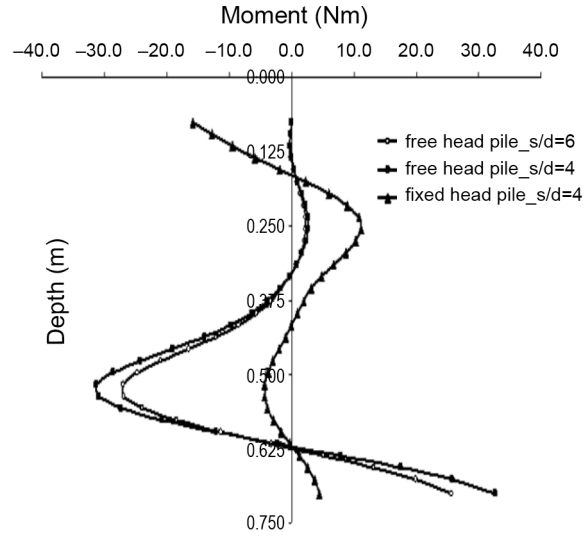

Fig. 10. Bending Moment Distributions at the 18 mm box displacement

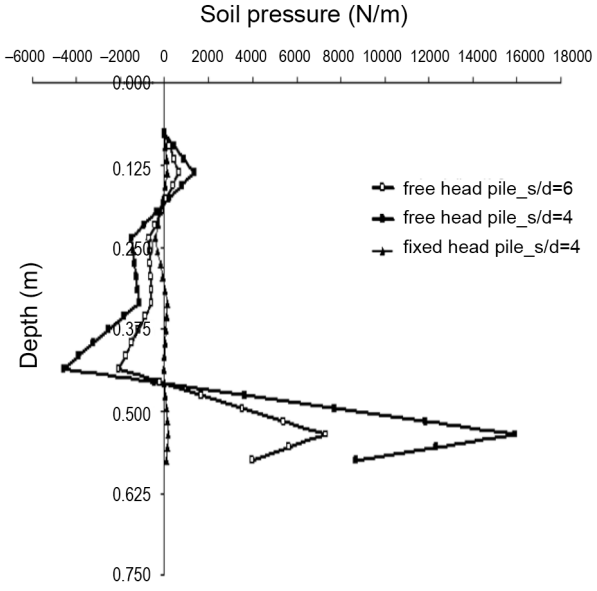

Fig. 11. Soil pressure distributions at the 18 mm box displacement

The bending moment and soil pressure distributions along the pile length evaluated from the bending strain data are given in Figs 10 and 11, respectively. It can be seen from figures that the maximum values of moment is increased with the decrease of pile spacing (Fig. 11). Soil pressure distribution obtained from the bending strain data confirms the existence of positive passive pressure zone. It can be observed that pile head movement exceeds the soil movement, resulting in positive passive pressure on the piles over a certain depth (i.e. approximately 20% of the sliding soil thickness). Below this depth, negative passive pressure occurs up to approximately 80% of the sliding soil thickness, and again positive passive pressure starts (Fig. 11). The maximum positive passive pressure has been observed nearly three fold of the maximum negative passive pressure. The pressure distribution increases with decreasing pile spacing.

6.2. Fixed head piles

As the displacement of the soil increases, loads acting on the fixed head piles increase rapidly as a result of load transfer mechanism like in the case of free head piles (Fig. 9). It is also revealed that the restrained pile head condition causes a decrease of the carried load per pile. It can be noticed from the Fig. 10 that the fixed head condition results in the smallest bending moment in the piles. The maximum bending moment in free head piles is about two times that in fixed head piles. It can be seen from Fig. 11 that the maximum value of soil pressure in the case of fixed head is less than that in free head piles. The relative displacements of the tracking points for fixed head piles with s/d = 4 were shown in Fig. 12. For the fixed head condition, piles resist against sliding and reduce the surficial soil displacements in contrast to the case of free head piles. Therefore, soil particles in the pile affected zone have less surficial displacements than the box displacement. Soil particles having less displacement than the box appear to displace towards the upslope direction in the time lapse images due to the resistance against sliding. The relative displacements of soil particles decreased with distance from the piles to the upslope direction.

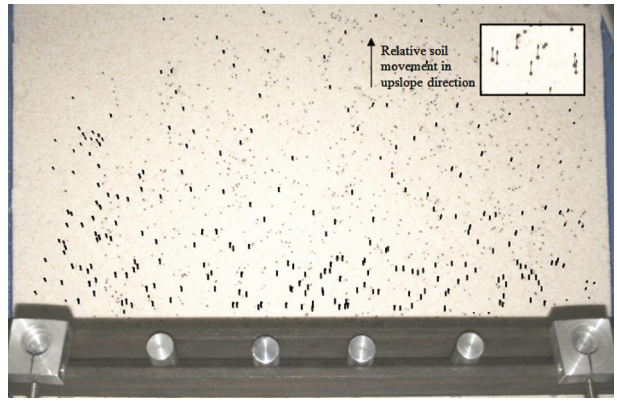

Fig. 12. The overall relative soil surface displacements throughout the test

The measured relative displacements were added to the box displacement in order to determine the magnitude and the direction of soil particle movement (Fig. 13). By connecting the soil particles having the same and the minimum surficial displacements, paths resembling arches can be established. The surficial displacement of soil particles located over the developed arches increased towards the upslope direction, similarly that below the arches increased towards the downslope direction as shown in Fig. 13.

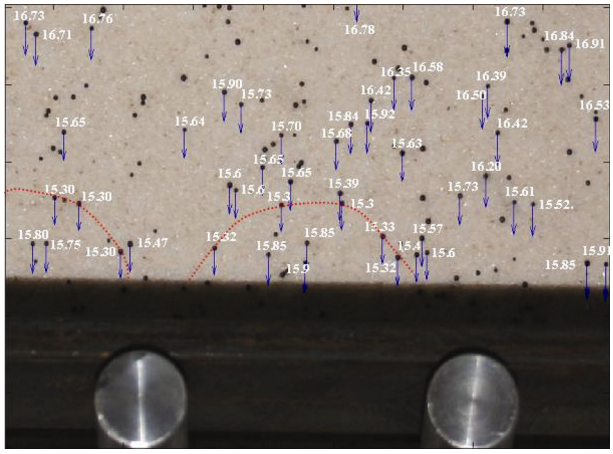

Fig. 13. Total soil surface displacements in mm due to soil arching with 18 mm box displacement

7. Conclusions

In this study, the load transfer mechanism in one row of slope stabilizing piles was investigated and discussed based on the experimental results. From the outcomes of this study, the following conclusions are drawn:

The behavior of the passive pile was significantly influenced by the pile head boundary conditions. For the case of free head pile, pile head movement exceeds the soil movement, resulting in positive passive pressure on the piles over a certain depth. Thus, the soil arching, which was determined from the load-displacement relations, was not observed on the soil surface. For the case of fixed head pile, soil particles in the pile affected zone have less surficial displacements than the box displacement. The surface displacement of soil particles located over the arches developed by connecting the soil particles having the same minimum surfacial displacements, increased towards the upslope direction, similarly that below the arches increased towards the downslope direction. This displacement behavior of soil particles are an evidence of the existence of soil arching mechanism on the soil surface.

It is more possible for the piles to be yielded by bending moment than by the shear force, a restrained pile head is recommended, and the free head condition should be avoided due to its relatively large bending moment acting on the piles. A restrained head condition can be obtained by connecting the pile heads with a buried beam, which is fixed by the tie-rods or tension anchors. If the restrained head condition cannot be obtained, the pile spacing should be decreased.

References

Adachi, T.; Kimura, M.; Tada, S. 1989. Analysis on the preventive mechanism of landslide stabilizing piles, in *Third International Symposium on Numerical Models in Geomechanics*, 8–11 May, 1989, Niagara Falls, Canada, 691–698.

Amšiejus, J.; Dirgėlienė, N.; Norkus, A.; Žilionienė, D. 2009. Evaluation of soil shear strength parameters via triaxial testing by height versus diameter ratio of sample, *The Baltic Journal of Road and Bridge Engineering* 4(2): 55–60.

Bosscher, P. J.; Gray, D. H. 1986. Soil arching in sandy slopes, *Journal of Geotechnical Engineering* ASCE 112(6): 626–645. http://dx.doi.org/10.1061/(ASCE)0733-9410(1986)112:6(626)

Cai, F.; Ugai, K. 2003. Response of flexible piles under laterally linear movement of the sliding layer in landslides, *Canadian Geotechnical Journal* 40(1): 46–53. http://dx.doi.org/10.1139/t02-103

Chelapati, C. V. 1964. Arching in soil due to the deflection of a rigid horizontal strip, in *Proc. of Symposium on Soil-structure Interaction*, 8–11 June, 1964, Arizona, University of Arizona, 356–377.

Chen, L. T.; Poulos, H. G.; Hull, T. S. 1997. Model tests on pile groups subjected to lateral soil movement, *Soils and Foundations* 37(1): 1–12. http://dx.doi.org/10.3208/sandf.37.1

Chen, C.-Y.; Martin, G. R. 2002. Soil-structure interaction for landslide stabilizing piles, *Computers and Geotechnics* 29(5): 363–386. http://dx.doi.org/10.1016/S0266-352X(01)00035-0

Christopher, M.; Geiger, G.; Liang, R., Yamin, M. 2007. Design methodology for drilled shafts to stabilize a slope, in *The 1st North American Conference*, 25–27 January, 2007, East Lansing, Michigan, USA. CD-form.

Cox, W. R.; Dixon, D. A.; Murphy, B. S. 1983. Lateral load tests of 25.4 mm. diameter piles in very soft clay in side-by-side and in-line groups, in *ASTM: SPT835 Laterally Loaded Deep Foundations: Analysis and Performance*. 18 p.

Davie, J. R.; Sutherland, H. B. 1978. Modeling of clay uplift resistance, *Journal of the Geotechnical Engineering Division* ASCE 104(6): 755–760.

Evans, C. H. 1983. *An examination of arching in granular soils*. MS Thesis. Department of Civil Engineering, Massachusetts Institute of Technology.

Gudehus, G.; Schwarz, W. 1985. Stabilization of creeping slopes by dowels, in *Proc. of the 11th International Conference on Soil Mechanics and Foundation Engineering*, 12–16 August, 1985, San Francisco, USA, 1697–700.

Hong, W. P.; Han, J. G. 1996. The behavior of stabilizing piles installed in slopes, in *Proc. of the 7th International Symposium on Landslides*, 17–21 June, 1996, Rotterdam, 1709–1714.

Iglesia, G. 1991. *Trapdoor experiments on the centrifuge: A study of arching in geomaterials and similitude in geotechnical models.* PhD Thesis. Department of Civil Engineering, Massachusetts Institute of Technology.

Ito, T.; Matsui, T. 1977. The effects of piles in a row on the slope stability, in *Proc. of the 9th I.C.S.M.F.E., Specialty Session*, 1977, Tokyo, Japan, 81–86.

Kahyaoğlu, M. R. 2010. *A modeling study for load transfer mechanisms of slope stabilizing piles*. PhD Thesis, The Graduate School of Natural and Applied Sciences of Dokuz Eylül University, İzmir, Turkey.

Kahyaoglu, M. R.; Imancli, G.; Ozturk, A. U.; Kayalar, A. S. 2009. Computational 3D finite element analyses of model passive piles, *Computational Materials Science* 46(1): 193–202. http://dx.doi.org/10.1016/j.commatsci.2009.02.022

Ladanyi, B.; Hoyaux, B. 1969. A study of the trapdoor problem in a granular mass, *Canadian Geotechnical Journal* 6(1): 1–14. http://dx.doi.org/10.1139/t69-001

Liang, R.; Zeng, S. 2002. Numerical study of soil arching mechanism in drilled shafts for slope stabilization, *Soils and Foundations* 42(2): 83–92. http://dx.doi.org/10.3208/sandf.42.2_83

Liang, R.; Yamin, M. 2010. Three-dimensional finite element study of arching behavior in slope/drilled shafts system, *International Journal for Numerical and Analytical Methods in Geomechanics* 34(11): 1157–1168.

Matsui, T.; Hong, W. P.; Ito, T. 1982. Earth pressures on piles in a row due to lateral soil movements, *Soils and Foundations* 22(2): 71–81. http://dx.doi.org/10.3208/sandf1972.22.2_71

Nalçakan, M. S. 1999. *Stabilization of landslides by piles in cohesive soils with special reference to group action reduction*. Ph.D. Thesis in Civil Engineering, Middle East Technical University, Ankara, Turkey.

Otsu, N. 1979. A threshold selection method from gray-level histograms, *IEEE Transactions on Systems, Man, and Cybernetics* 9(1): 62–66. http://dx.doi.org/10.1109/TSMC.1979.4310076

Pan, J. L.; Goh, A. T. C.; Wong, K. S.; Teh, C. I. 2000. Model tests on single piles in soft clay, *Canadian Geotechnical Journal* 37(4): 890–897. http://dx.doi.org/10.1139/t00-001

Pan, J.; Goh, A.; Wong, K.; Teh, C. 2002. Ultimate soil pressures for piles subjected to lateral soil movements, *Journal of Geotechnical and Geoenvironmental Engineering* ASCE 128(6): 530–535. http://dx.doi.org/10.1061/(ASCE)1090-0241(2002)128:6(530)

Poulos, H. G. 1996. Design of reinforcing piles to increase slope stability, *International Journal of Rock Mechanics and Mining Sciences and Geomechanics Abstracts* 33(5): 225A–226A. http://dx.doi.org/10.1016/0148-9062(96)80104-5

Reese, L. C.; Wang, S. T.; Fouse, J. L. 1992. Use of drilled shafts in stabilizing a slope, in *Proc. of Specialty Conference on Stability and Performance of Slopes and Embankments*, June 29–July 1, 1992, California, Berkeley, 1318–1332.

Sommer, H. 1977. Creeping slope in a stiff clay, in *Proc. of the 9th International Conference on Soil Mechanics Foundation Engineering*, 10–15 July, 1977, Tokyo, Japan, 113–118.

Thompson, M. J.; David, J. W.; Muhannad, T. S. 2005. Lateral load tests on small-diameter piles for slope remediation, in *Proc. of the 2005 Mid-Continent Transportation Research Symposium*, 18–19 August, 2005, Ames, Iowa, 1–13.

Verveckaite, N.; Amsiejus, J.; Stragys, V. 2007. Stress-strain analysis in the soil sample during laboratory testing, *Journal of Civil Engineering and Management* 13(1): 63–70.

Viggiani, C. 1981. Ultimate lateral load on piles used to stabilize landslides, in *Proc. of 10th ICSMFE*, Stockholm, Sweden, 1981, Vol. 3, 555–560.

Ždankus, N. T.; Stelmokaitis, G. 2008. Clay slope stability computations, *Journal of Civil Engineering and Management* 14(3): 207–212. http://dx.doi.org/10.3846/1392-3730.2008.14.18

Zeng, S.; Liang, R. 2002. Stability analysis of drilled shafts reinforced slope, *Soils and Foundations* 42(2): 93–102. http://dx.doi.org/10.3208/sandf.42.2_93

Zhao, M. H.; Liu, D. P.; Zhang, L.; Jiang, C. 2008. 3D finite element analysis on pile-soil interaction of passive pile group, *Journal of Central South University of Technology* 15(1): 75–80. http://dx.doi.org/10.1007/s11771-008-0016-9

Mehmet Rifat KAHYAOĞLU. Assistant professor in Department of Civil Engineering, at Muğla University, Merkez-Muğla, Turkey. His research interests: passive piles, slope stabilization and geosynthetics.

Okan ONAL. Assistant professor in Department of Civil Engineering, at Dokuz Eylul University, Buca-İzmir, Turkey. His research interests: digital image processing, artificial neural network applications.

Gökhan IMANÇLI. Research assistant in Department of Civil Engineering, at Dokuz Eylul University, Buca-İzmir, Turkey. His research interests: geomechanics of landfills and hydraulic conductivity of geosythetic clay liners.

Gürkan OZDEN. Associate professor in Department of Civil Engineering, at Dokuz Eylul University, Buca-İzmir, Turkey. His research interests: soil dynamics, soil-pile interaction.

Arif Ş. KAYALAR. Professor in Department of Civil Engineering, at Dokuz Eylul University, Buca-İzmir, Turkey. His research interests: soil mechanics, foundation engineering.